

# Chapter 4

## Organic Nanostructures by Molecular Layer Epitaxy: A Tutorial



Tatjana N. Kopylova, Sergey Yu Nikonov, Evgeny N. Telminov,  
Ruslan M. Gadirov, Konstantin M. Degtyarenko, and Vladimir Burtman

**Abstract** This chapter presents a short introduction to molecular layer epitaxy (MLE). MLE is a novel vapor-phase self-assembly approach to create molecular nanoelectronic materials, structures, and devices. The main principles of MLE technology and related topics of surface chemistry are introduced to demonstrate the possibilities of vapor-phase self-assembly, which can be used to achieve desired organic structures and chemical functionalities. We describe equipment, which can produce MLE structures, and monitoring methods used to describe growth of organic MLE structures. We demonstrate several devices, which were produced using MLE technology. These include field-effect transistors (MLE-FETs), organic light-emitting diode (MLE-OLED), MLE solar cells, and MLE laser media. The performance of MLE is compared with other technologies, which are currently used in molecular nanoelectronics, to demonstrate similarities and distinguish features of MLE.

### 4.1 Molecular Nanoelectronics

#### 4.1.1 *Molecular Nanoelectronics at Early Ages*

2017 marks the 20th anniversary of Mark Reed's article "Conductance of a molecular junction" on the possibility of electronic transport through a single molecule [1]. This was the first experimental step of molecular nanoelectronics, which was theoretically predicted by Aviram and Ratner in 1974 [2]. The initial expectations from molecular nanoelectronics were associated with ideas to combine advantages

---

T. N. Kopylova · S. Y. Nikonov · E. N. Telminov · R. M. Gadirov · K. M. Degtyarenko  
Siberian Physics and Technical Institute, Tomsk State University, Tomsk, Russia  
e-mail: [kopylova@phys.tsu.ru](mailto:kopylova@phys.tsu.ru)

V. Burtman (✉)  
University of Utah, Frederick Albert Sutton Building, 115 S 1460 E #383, Salt Lake City 84112,  
Utah, USA  
e-mail: [vlad.burtman@utah.edu](mailto:vlad.burtman@utah.edu)

of cheap production of organic materials and their structural flexibility with the possibility to create single molecular semiconductor devices. In the early 2000s, experimental molecular nanoelectronics continued to produce vivid results. For example, the possibility of creating transistors with multiple stable states (based on the rotoxane molecule [3]) was demonstrated. Articles on spin transport in organic molecules discussed the possibility of creating an entirely new class of materials for molecular spintronics [4] and molecular magnetism. First experiments, which study organic molecules as biological objects, such as DNA, proteins, and neurons, can yield bioelectronic devices, which can transmit biological signals and control processes in living organisms [5].

Unfortunately, the initial expectations for rapid progress in molecular nanoelectronic devices have not come true. For example, Samsung indeed released few years ago a new generation of monitors, which are based on organic light-emitting diodes (OLEDs). However, the production costs of OLEDs monitors were similar to these models, which utilized inorganic semiconductors. Attempts to create efficient organic-based solar cells have not come true as well, due to their high costs and low operation performance. Currently only hybrid types of organic-inorganic devices, like Gratzel cells [6] and hybrid perovskites cells [7], still hold high expectations for device application. In addition, it was found that several key researchers in molecular nanoelectronics falsified the results of their work [8], and others misinterpreted them. For example, the interpretation of transport through individual molecules in Reed's article [1] was found to be erroneous [9].

This situation in molecular nanoelectronics at early ages was not accidental. Scientists working in molecular nanoelectronics concentrated their efforts on developing breakthrough device applications, rather than on fundamental studies of single molecular materials. As a result, molecular nanoelectronics still struggles to develop an adequate model of charge transport in molecular nanoelectronic devices based on a single molecular structure. For more than 25 years, scientists have been trying to adapt various models of solid-state physics, which were developed for inorganic semiconductors. These transport models relies on possibility to consider electrons in inorganic semiconductor devices as free by using the concept of effective mass of electron. The fundamental difference between organic and inorganic semiconductors is in absence of free charges in organic media. Due to this fact, there are no conduction and valence bands in organic semiconductors. Instead of conduction and valence bands, molecular electronics utilizes terms HOMO-LUMO. These acronyms stand for "highest occupied molecular orbital" and "lowest unoccupied molecular orbital," respectively. The applicability of free-electron theoretical concept is a problem in single molecular media. The fundamental structure-property relationship in molecular structures remains unclear, which impede development of new materials and devices in molecular nanoelectronics. Eventually, after exploration of easiest approaches and disappointments from lack of fast progress in molecular nanoelectronics, many scientists left this field. The remaining scientist began to redefine the broader scope of problems to solve in molecular nanoelectronics, began to utilize more complex scientific approaches to describe experimental objects, and, overall, began to employ higher scientific standards in their research.

### ***4.1.2 Modern Times in Molecular Nanoelectronics***

In 2013 the whole volume of Nature Materials [10] was dedicated to experimental studies in molecular nanoelectronics. These studies show a good example of new approach to molecular nanoelectronics, which is way more complex and sophisticated compared to experimental reports in early year's studies. Nowadays molecular nanoelectronics is shaping as classical science, in which the development of practical applications is combined with fundamental studies of the structure and properties in individual molecules.

The other distinguishing feature of modern time in molecular nanoelectronics is associated with the fact that this field received scientific and financial support from biology and medicine. In particular, new high-level studies on electronic transport in biological objects, as in DNA molecules, have been published [11]. Biological molecule, like DNA, has a similarity in structure to molecules used in molecular nanoelectronics. Understanding the mechanisms of charge transport in biology will make it possible to make significant progress in understanding similar mechanisms in molecular nanoelectronics.

In year 2016, Google and the British pharmaceutical company GlaxoSmithKline created a bioelectronic company for the use of miniature electrical implants in the treatment of chronic brain diseases, with the potential for further development of the interface between the brain and electronics [12]. In 2017, an American businessman Elon Musk entered into a similar project aimed at establishing a connection between the brain and the computer [13]. In the context of this development, we should note that only molecular nanoelectronics can provide a reliable interface between biological objects (neurons, DNA, proteins, etc.) and traditional electronic materials, including metal electrodes and semiconductor devices. In addition to biotechnologies, the new challenges for molecular nanoelectronics appear every year. These challenges include the development of catalytic nanomembrane technology [14], which can be utilized in new device concepts as an "artificial leaf" technology which is capable of converting exhaust gases into fuel using the energy of sunlight and can be entitled as artificial photosynthesis. The other example of contemporary challenges for molecular nanoelectronics is design and development of new field-effect transistors (FETs). Example of new FET system is shown in this book in chapter "The FinFET: A Tutorial" by Charles Dančák. Once single molecular transistor will become a robust and scalable technology, it has a good chance to become a new basis for electronic logics.

### ***4.1.3 Quest for a New Fabrication Methods in Molecular Nanoelectronics***

Among the numerous methods for creating materials with specified properties in molecular nanoelectronics, we should mention the methods of so-called "wet" and "vacuum methods." The wet methods include Langmuir films [15], self-assembling

monolayers [16], and assembly of structures from solutions based on electrostatic interactions [17]. The vacuum methods include organic molecular beam epitaxy [18], other high-vacuum methods, and low-vacuum gas-phase deposition techniques, known as CVD technologies. Wet and vacuum methods have their advantages and disadvantages.

For example, “wet” methods are able to create stronger chemical bonds between organic layers, in differ to traditional methods of producing nanoelectronic structures from the “vapor” phase. However, the “wet” methods are very time-consuming and in their structure always contain a residual of solvents, which are able to affect the entire efficiency of the device. In addition, a number of interesting but insoluble organic substances cannot be used by “wet” chemistry.

Vacuum methods for creating stratified structures from the gas phase are capable of applying organic films quickly and in a clean atmosphere. They are fully compatible with modern semiconductor technologies. However, none of them is capable of creating strong covalent bonds between the layers, which limits the scope of the structures obtained. The main drawback of modern molecular nanoelectronic devices is instability. They are unstable for long periods of use, at elevated temperatures, with strong electric fields, unstable so that often even the spraying of electrodes presents a problem. The reason of these problems is the weak links inside the resulting films.

#### ***4.1.4 From Atomic Layer Epitaxy to Molecular Layer Epitaxy***

The main precondition for the device application of organic structures is the combination of epitaxial growth with covalent bonding in some similarity to the case of vapor deposition of inorganic semiconductors. The term *epitaxy* comes from combination of two Greek words: *epi* and *taxis*, which translates as “upon” and “arrangement.” Therefore, the meaning of *epitaxy* is “ordering above,” which simply means that the structure of the first layer defines the structure of the second layer. Many phenomena in chemistry, biology, crystal growth, geology, and material science are controlled by epitaxy; for example, the self-assembly process of fluids to form SAMs on metals. Some organic ultrahigh vacuum (UHV) [19] and organic molecular beam epitaxy (OMBE) methods [20] succeed in epitaxial growth, and some solution-derived SAMs can form interlayer covalent bonds. However, only inorganic atomic layer epitaxy (ALE) [21] can build covalently bonded epitaxial multilayers in a layer-by-layer fashion. The term *epitaxy* in ALE method means that the structure of upper layer is completely defined by bottom layer in ALE structure. While there are no strict terminology rules, the term *epitaxy* usually refers to the vapor-phase assembled structures, with strong (e.g., covalent) bonds between adjacent layers. When the structure is assembled using weak bonds (e.g., WdW bonds), the term *epitaxy* is used as a *pseudo-epitaxy* [16].

The ALE approach utilizes the difference between chemical and physical adsorption. When the first layer of atoms of a reactive molecular species reaches a

solid surface, a chemical reaction (generally condensation) takes place, while subsequently deposited physisorbed layers tend to interact much less strongly. If the substrate surface is heated sufficiently, one can achieve a condition such that only the chemisorbed layer remains attached. Repeating this reaction cycle with different compounds leads to a controlled layer-by-layer growth. The ALE method was successfully applied to the epitaxial growth of “conventional” semiconducting inorganic materials, such as II–VI and III–V compounds and silicon and silicon-related compounds (see molecular beam epitaxy, atomic layer epitaxy).

A new method, molecular layer epitaxy (MLE) [22], has been developed for the deposition of organic heterostructures. In contrast to most ordered organic SAM thin films that are assembled in solution, the MLE approach employs a low-pressure vapor-phase epitaxial growth via covalent bonds between organic interfacing layers. Term epitaxy in MLE method designates organic structures based on strong bonds, which bonding energy above 1.8 eV.

## 4.2 Methodology of Molecular Layer Epitaxy

### 4.2.1 MLE Principles and Hardware

The MLE method is based on four principles: a template layer, self-restricted vapor-phase reactions, covalent (“c-axis”) interlayer bonding, and  $\pi$ -stacking in the x-y plane (the plane of the substrate). The MLE method is based on the use of modern equipment for rapid and clean application of organic layers (Figs. 4.1 and 4.2), but unlike other “gas” methods, MLE allows for chemical self-assembly of layers with the formation of strong covalent bonds between them. The technology is based on the successive growth of a layer on the surface of a substrate from individual molecules of vapors of a heated organic substance. Specially designed for MLE vacuum system was developed and assembled on the basis of the most modern thin film technology. This unit heats the precursor materials to high temperatures

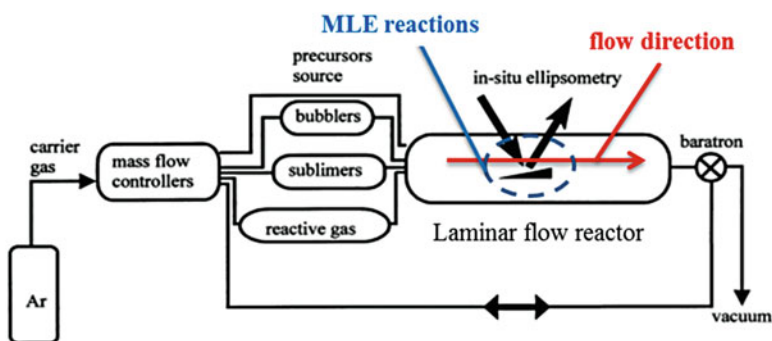


Fig. 4.1 Scheme of laminar flow MLE reactor setup



**Fig. 4.2** Photograph of 2nd generation of molecular layer epitaxy setup

(500 °C) in a vacuum ( $10^{-5}$  Torr). The evaporated molecules are trapped in a special way and placed on the substrate layer by layer, forming the thinnest film (*c.a.* 3 nm).

The second generation of MLE setup (Fig. 4.2) inherits from the first generation of MLE setup [22] the similar shape of CVD chamber and position of its functional elements (sublimators, bubblers, pumps etc). It featured an addition of few high-temperature sublimators and higher reactor temperature and pressure. These additions enable usage of high-temperature precursor materials and using vapor-phase self-assembly reactions at higher temperatures. The ultimate goal of 2nd generation MLE setup was to gain a realistic possibility to include inorganic precursor materials in MLE chemical routine to produce mixed organic-inorganic superlattices within the same reactive chamber. The other additions to 2nd generation of MLE setup include better temperature, pressure and evaporation control, and an easy-to-set automatic operation mode to illuminate necessity in direct manual operation of MLE process.

These artificial submicron organic structures are characterized by a high degree of ordering and strong covalent bonds between the layers, as shown in Fig. 4.3.

#### ***4.2.2 Examples of MLE Chemistry with Different Chemical Functionality on Top***

##### **MLE with Top Amino-Group Chemical Functionality**

The surface chemistry of the MLE method, as shown in Fig. 4.4, allows the growth of naphthalene-diimide-based organic structures.

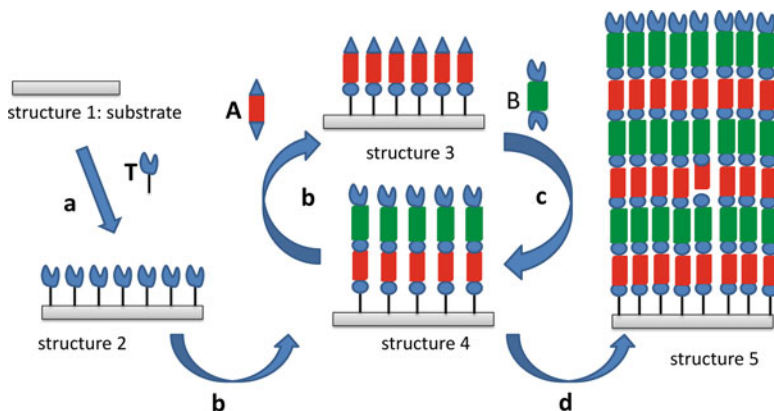


**Fig. 4.3** Molecular layer epitaxy (MLE) method: organization of structures, when the structure of the upper layer is controlled by the structure and chemical composition of the previous layer. The figure shows the scheme of epitaxy. First, the “anchor layer” (arrow “a”) is placed on substrate 1 (the arrow “a”); structure 2 is formed. Next, a layer of molecules A (arrow “b”) is applied on 2; a structure 3 with two assembled layers is formed. Next, a layer of molecules B (arrow “c”) is applied; a structure 4 is formed. Thus, it is possible to assemble a structure of necessary thickness with alternating layers (arrow “d”)—a superstructure 5 is formed. It is essential that layer A is adapted to accept layer B, and vice versa, it is impossible to collect more than one layer only A or only B

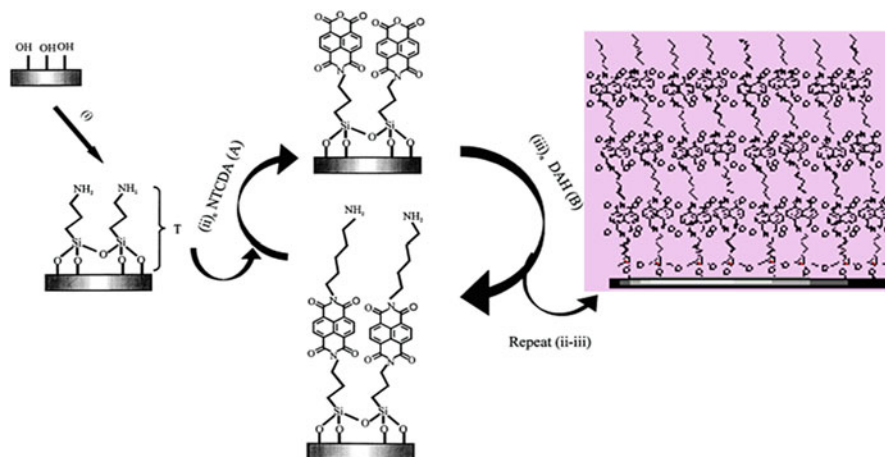


**Fig. 4.4** MLE surface chemistry with amino group on top of MLE structure

A template layer is first deposited on oxide surfaces, such as Si/SiO<sub>2</sub> (Fig. 4.4, step i), exposing propylamine functionality toward the interface, and in turn this layer dictates epitaxial growth. Then discrete pulses of reactants—liquids or solids that undergo self-limiting reactions—are carried to the surface by an inert carrier gas

in a laminar flow MLE reactor setup (Reynolds number  $\sim 250$ ) (Fig. 4.2) equipped with a spectroscopic ellipsometer for in situ process monitoring. An alkylamine-containing surface is hit with a pulse of 3,4,7,8-naphthalenetetracarboxylic-dianhydride (NTCDA) precursor (Fig. 4.4, step ii), forming imide linkages. Then a pulse of a vaporized aromatic or aliphatic diamine spacer (Fig. 4.4, step iii) is added to regenerate amine functionality on the surface that can again react with dianhydride.

Repeatedly cycling through these steps (Fig. 4.4, steps ii,iii) leads to the formation of a 3,4,7,8-naphthalenetetracarboxylic diimide (NTCDI)-based organic superlattices. The NTCDA precursor was vaporized at  $T = 200\text{--}250\text{ }^\circ\text{C}$  to react with the surface-bound amine; 1,6-diaminohexane and 4,4'-methylenedianiline precursors were vaporized at  $T = 35\text{--}40\text{ }^\circ\text{C}$  and  $90\text{--}110\text{ }^\circ\text{C}$ , respectively. Imidization in both steps is carried out at a substrate temperature of  $280\text{--}290\text{ }^\circ\text{C}$  for 15–25 min at a total pressure of 0.05 torr. Following the assembly of each monolayer, the reaction zone is cleaned by resublimation of unreacted precursors under  $\text{N}_2$  flow for 5 minutes. The reactor walls are independently heated to  $300\text{ }^\circ\text{C}$ .

### MLE with Top Thiol Group Chemical Functionality

Fabrication of different molecular electronic devices usually requires different chemical functionality. In particular, thiol functionality is often required for formation of chemical bonds with upper metal electrodes (Au, Ag, Al, etc.). Chemical approach to MLE assembly of naphthalenetetracarboxylic diimide (NTCDI) self-assembling structure with thiol group on top is highlighted in Fig. 4.5. The first step (*a*) of the process is the assembly of a template layer containing primary amine functionality. This process can be conducted either from solution or vapor phase. The multilayer growth is done with the MLE reactor. The first pulse of substrate (Fig. 4.5, step *b*) is a dianhydride reaction with the exposed amine functionality of the template layer forming an imide bond and exposing anhydride functionality at the emerging interface. The following step (*c*) anchors diamine containing precursors (spacers) again by the formation of an imide bond and exposing thiol functionality on top. Molecular 2D surface aggregates, stage (*d*), grow orthogonally to planar view of NTCDI molecule, shown between stages (*b*) and (*d*).

NTCDI-based structures were accomplished as follows. Thick, impermeable to light, wafers of n-type ( $500\text{ }\Omega\text{-cm}$ , Virginia Semiconductors) Si(100) having  $20\text{ }\text{\AA}$  of  $\text{SiO}_2$  coating and glass slides were cleaned and functionalized with amino groups (Fig. 4.5, step *a*) as described in ref. 17. NTCDA (1,4,5,8-naphthalene tetracarboxylic anhydride) evaporated at  $110\text{ }^\circ\text{C}$  and reacted with the  $\text{NH}_2$ -functionalized surface for 45 min at  $10^{-5}$  Torr (Fig. 4.5, step *b*). The product of assembly lacks the amino group preventing formation of the second layer. The substrate was kept on a heated sample holder ( $180\text{ }^\circ\text{C}$ ) preventing physisorption of the precursor. Vacuum deposition modified over 60% of the surface amino groups [17]. A layer of 4-aminophenylthiol was added within 20 min (Fig. 4.5, step *c*). This reaction tops the surface with SH-groups reactive toward metals [23].



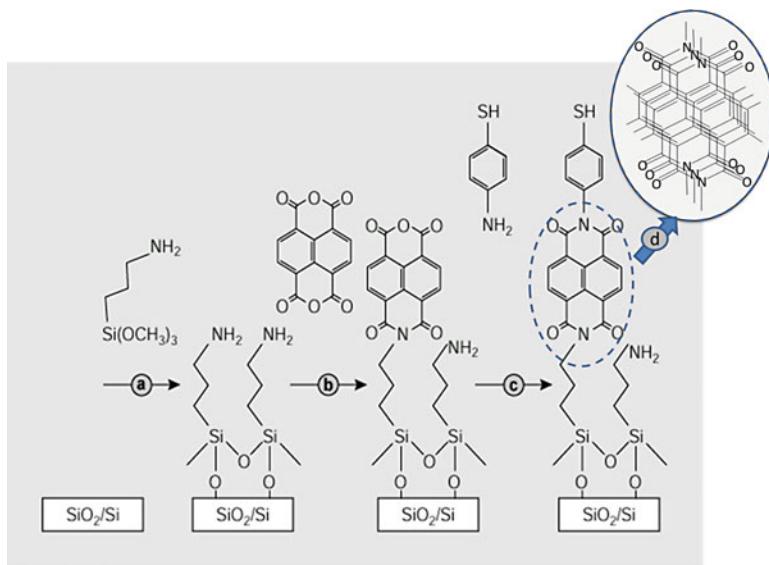


**Fig. 4.5** Surface chemistry, which yields surface  $\pi$ -aggregation system in naphthalenetetracarboxylic diimide (NTCDI) system by molecular layer epitaxy (MLE) method with a thiol group on top. The NTCDI aggregates may be visualized as structures that are orthogonal (*out-of-plane*) to picture plane, as shown in right upper corner

The control experiments to verify the quality of vapor-phase self-assembly include spectroscopic in situ and ex situ ellipsometry, measuring progressive contact angle, XPS, and recording of absorption spectra after deposition of each layer [24].

### 4.2.3 Monitoring Tools to Trace the Growth of Organic Superlattices

#### Monitoring of Growth of Organic Superlattices by Spectroscopic Ellipsometry

Experimental setting for in situ spectroscopic ellipsometry monitoring the MLE process is shown in Fig. 4.6. This figure highlights position of Woollam M44 spectroscopic ellipsometer, including position of optical windows, substrate, and reactive zone, in respect to axis of MLE reactor, precursor and carrier gas flow, vacuum, and unreacted products. The  $\phi$  angle is a spatial angle between incoming linearly polarized light and orthogonal to reflection point on substrate in the plane of incidence. Linearly polarized light become circularly polarized after reflecting from MLE structure, which is grown on the substrate in real time (Fig. 4.6). In ellipsometry light, which vector of electrical field oscillated within the plane of incidence is called *p*-polarized light, and light, which vector of electrical field

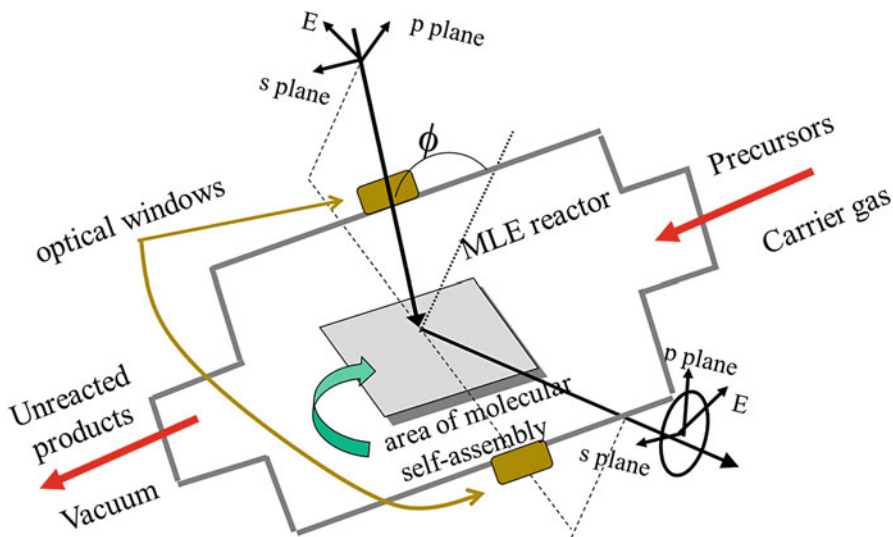


**Fig. 4.6** Experimental setting for in situ spectroscopic ellipsometry monitoring the MLE process

oscillated perpendicular to the plane of incidence is called *s*-polarized light. The basic principles of ellipsometry rely on the fact that *s*- and *p*-polarized light reflect differently:  $R_p \neq R_s$ . The ellipsometry measures the complex reflectivity ratio,  $R_p/R_s = \tan(\psi)e^{i\Delta}$ , and typically reports results in terms of  $\psi$  and  $\Delta$  parameters. The  $\tan(\psi)$  is a magnitude of the  $R_p/R_s$  ratio and  $\Delta$  is a phase difference between *p*- and *s*-reflected light. We study the evolution of ellipsometry parameter  $\psi$ , which changes in real time and reflects the change of light polarization upon different stages of self-assembly reaction and growth of organic superlattice.

Figure 4.7 shows an example of MLE process monitoring for continuous growth of naphthalenetetracarboxylic diimide-hexamethylene (NTCDI-HM)<sub>n</sub> structure,  $n = 4$ , assembling from NTCDA and DAH precursors in single wavelength representation. This figure shows the change in the surface polarization parameter  $\psi$ , detected by in situ ellipsometry versus deposition time.

The temporal evolution of the monolayers by in situ ellipsometry provides several interesting observations. First, the ellipsometry parameters  $\psi$  and  $\Delta$  are very sensitive to the surface prefunctionalization. Even the raw data exhibit the periodical growth and decay of surface polarizability at different steps of the ML-assembling process with periods of about 15 minutes for the NTCDA pulse and 18 minutes for the DAH pulse. Figure 4.7 also provides information on the kinetic behavior of the self-assembly process since  $\psi$  and  $\Delta$  can be converted to surface chromophore or spacer-relative coverage. The rate coefficients  $k$  for every pulse are  $5.6 \times 10^{-5} \text{ s}^{-1}$  for first deposition of NTCDA on a template layer, decreasing to  $1.5 \times 10^{-5} \text{ s}^{-1}$  for NTCDA on a hexamethylene layer and to  $7.2 \times 10^{-6} \text{ s}^{-1}$  for DAH on a naphthalene layer with an equilibrium surface absorption energy 15.8 kcal for the NTCDA layer and 29.2 kcal for the DAH layer.

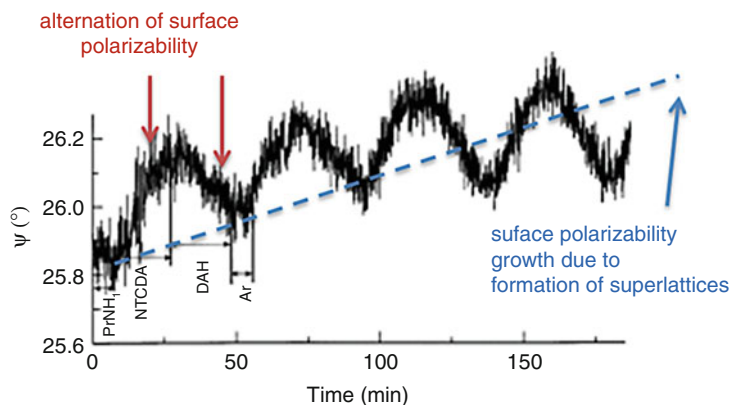


**Fig. 4.7** In situ monitoring of MLE monolayer-by-monolayer growth

The in situ (Fig. 4.7) and ex situ [19] ellipsometry measurement is a very useful tool in monitoring of MLE-derived structures, especially for cases in which different building blocks of organic superlattice have a different molecular polarizability, as in case of NTCDI-HM system.

The ex situ spectroscopic ellipsometry can be useful for structural analysis of MLE superlattices [19]. However, ex situ spectroscopic ellipsometry is less illustrative and requires knowledge of optical constants ( $\epsilon$  and  $n$ ) for each consistent layer to build an adequate model for MLE structure.

### Monitoring of Growth of Organic Superlattices by Optical Spectroscopy

Monitoring of growth of organic superlattices by optical spectroscopy is one of the simplest and very sensitive tools to ensure a consistent growth of MLE-derived organic superlattices. The precondition for using this monitoring method consists in usage of sensitive spectrophotometer with spectral resolution of optical density (OD) about 0.001. This resolution has to resolve the growth of one monolayer. The other technological complication for this (ex situ) method is the necessity to interrupt MLE process to record Vis-UV spectra and then to continue MLE process. This approach might be problematic for a range of materials and technologies, including, for example, air-sensitive materials. In situ reflection optical spectroscopy monitoring should resolve this complication. However the alignment of in situ optical instrumentation might be complicated, especially taking into account the necessity of high OD sensitivity.

The structure of organic superlattices, which is traced by ex situ *UV-Vis* optical spectroscopy, is shown in Fig. 4.8. This figure provides an easy access to understand the main spectral features, which should be traced to ensure the quality self-assembly in vapor phase. Figure 4.8 shows a monolithic growth of the ten bilayer superlattice containing aliphatic spacer in the absorption at 362 nm. We designated this band as a

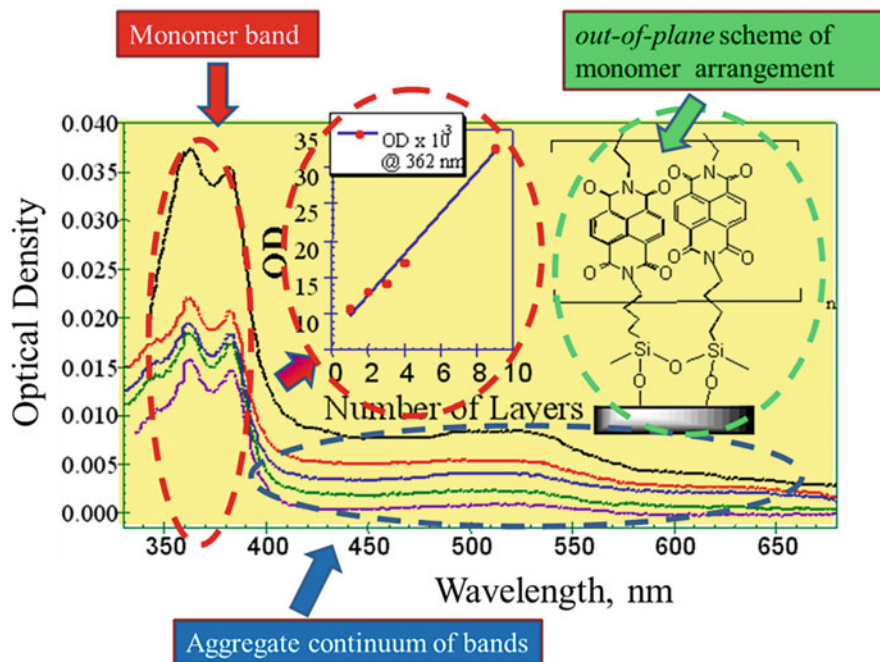


**Fig. 4.8** The structure of organic superlattices, which is traced by UV-Vis optical spectroscopy: absorption spectra of MLE-derived (NTCDHI)<sub>n</sub>-based organic superlattice for  $n = 1, 2, 3, 4, 9$ . Different spectral features are specified in form of colored dashed lines, arrows, and text boxes

“monomer band” (red text box, arrows, and dashed lines). The middle panel in Fig. 4.8 shows the monotonic growth (blue line in the middle insert) of optical density at 362 nm of this “monomer band.” The *out-of-plane* structure of growing NTCDI-organic superlattice is shown in the right upper insert (green dash line and green text box). Note that for graphic simplicity we do not show here the *in-plane* order in NTCDI-organic superlattice. The *in-plane* packing inside one NTCDI layer in NTCDI superlattice is shown in upper right part of Fig. 4.5.

The intermolecular charge transfer (CT) band is observed around 450–700 nm exhibiting the high *in-plane* packing density. We designated this band as an “aggregate continuum of bands” (blue text box, arrows, and dashed line). This band is originated from delocalization of  $\pi$ -electrons in aromatic rings during aggregation of NTCDI moieties into clusters, in which these electrons become pseudo-conductive in narrow continuum of bands (COB) [25].

To verify the quality growth of organic superlattices, the main attention has to be paid to tracing of growth of OD of monomer band (362 nm, Fig. 4.8). These spectra are recorded after each step of self-assembly reaction and measuring the absorption spectra. The growth of OD should be of order of  $\sim 0.001$  for adding of next layer, this growth should be consistent and such growth should be linear in first approximation. Any inconsistency in monitoring spectra in form of much lower or much

higher increment of OD for any grown layer, or change in shape of monomer band, or sharp shift of monomer band (362 nm) to blue or red region is a clear indication of problems in growth of organic superlattices. Most common problem in MLE process is interruption in growth of OD, which indicates problem in MLE growth. Despite difficulties, which are noted in the beginning of this section, the monitoring of growth of organic superlattices by optical spectroscopy is still very efficient for adjustment stage of MLE technology for any new material system.

The distinguished feature of spectroscopic ellipsometry and UV-Vis spectroscopy consists in their capability to trace not only the fact of molecular self-assembly in vapor phase but also to evaluate the molecular density in each consistent layer. This is particularly useful to avoid the problem of pyramidal growth, which is typical for solution molecular self-assembly.

### **Other Monitoring Methods Used to Describe the Grow of Organic Superlattices**

The monitoring of nonlinear response from growth organic structures can be used to trace in real time as well in certain cases. For example, the measurement of second harmonic generation (SHG) response from organic superlattices, which contain the molecules with SHG response, can be used to trace their growth [26]. The list of simple and sensitive tools to trace the growth of organic superlattices includes measurement of progressive contact angle after each step of self-assembly reaction. FTIR spectroscopy is another useful tool to trace chemistry of substituted amine (substitution of oxygen in NTCDA ring to nitrogen) during MLE growth [22]. These monitoring tools today cannot be used directly to evaluate the package density within each consistent layer and, therefore, can be employed as quality tools.

We impose in this section that increment in spectroscopic and polarization response from growing organic superlattice can be considered additive in first approximation. This includes the monotonic growth of polarization and optical densities in Fig. 4.7 (blue-dashed trend line) and Fig. 4.8 (blue trend line in the middle insert of optical density at 362 nm). This assumption is well enough for a general monitoring purpose. However, the close look on dependence increment in spectroscopic and polarization response from growing organic superlattice (e.g., growth of OD with number of monolayers,  $n$ , see Fig. 4.8) reveals nonlinearity at  $n > 10$ . This nonlinearity is attributed to size-dependent effects in organic superlattices. The measurement of size-dependent effects in organic structures using absorption spectroscopy along with electro-optical properties of MLE structures is discussed in the following section.

#### 4.2.4 Size-Dependent Effects in MLE Structures

Accounting the size-dependent effects in MLE structures might be critical in some situations, for example, when a good *in-plane* density of MLE films becomes critical and the number of contained monolayers  $n$  exceeds ten ( $n > 10$ ). Example of devices, which may contain such structures, includes planar photovoltaic cells, with capability to harvest light excitation from macroscopic distances, or MLE-FET devices. In these cases the size-dependent effect should be accounted to ensure an adequate accuracy of structural evaluation.

However, this remarkable feature of superlattices is a topic of independent scientific interest. The size-dependent characteristic in NTCDI-based superlattices can be studied by their optical absorption signature. The blueshift in the absorption peak corresponding to an increase in transition energy  $\Delta E$ , predicted as the thickness of the multilayer decreases, was observed for a range of organic and inorganic superlattices. The same trend is observable in the lowest-energy absorption peak of the MLE-derived NTCDI superlattices, depicted in Fig. 4.9a. An energy decrease of about 12 meV is measured for the multilayered structures containing the fewest layers of NTCDI with aliphatic HM spacers. Considering the organic multiple quantum well (OMQW) energy levels to consist of NTCDI (a) semiconducting narrow potential wells placed in between very high-potential barriers (b) (aliphatic spacers), both electron and hole can be approximated as confined in the NTCDI layer. Then a model of a confined Wannier exciton in coupled quantum wells can be considered. The exciton binding energy ( $E_{1s} = \langle \psi | H | \psi \rangle$ ) was determined to fit the blueshifted absorption peak, shown as a dashed line in Fig. 4.9a.

Variety of other spectroscopic tools can be employed to study the growth of MLE structures. For example FTIR spectroscopy is capable to trace the chemical reaction, in which surface amine react with NTCDA anhydride to produce the imide interlayer bonding [27].

### 4.3 MLE-Derived Molecular Nanoelectronic Devices

#### 4.3.1 MLE Field-Effect Transistors (MLE-FETs)

The MLE-derived devices' operation stability is robust and able to operate at a DC field of  $3 \times 10 \text{ Vcm}^{-1}$ . This stability, unusual for organic devices, can be explained by the energy of imide bonds that is about 1 eV in contrast to that of van der Waals bonds (0.01 eV) achieved by most solution and ultrahigh vacuum (UHV) deposition methods. The possibility to achieve controlled epitaxial ML growth and ohmic contacts on an inorganic-organic level enables us to fabricate stable and highly ordered molecular electronic devices as OFETs and organic single-electron

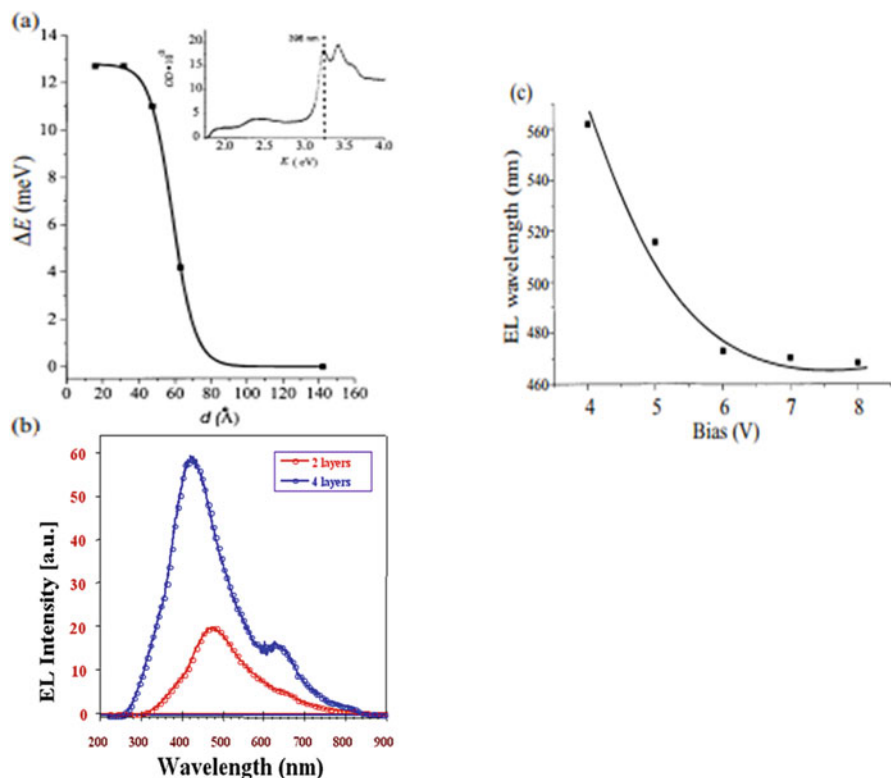


**Fig. 4.9** Scaling laws for MLE-derived organic superlattices: (a) Energy shift of the NTCDI-HM superlattice absorption peak, marked by the arrow in the insert graph, as a function of thickness. The symbols correspond to experimental data, and the solid curve is the fit to model described in the text. Insert: Absorption spectrum of  $(\text{NTCDI-HM})_2$  multilayer sample. (b) Thickness-dependent EL in  $(\text{NTCDI-DPM})_n$  for  $n = 2$  and 4 in MLE-based OLED at VDC = 8 V. (c) DC voltage-dependent EL for  $(\text{NTCDI-DPM})_4$ -based OLED

transistors. 1,4,5,8-Naphthalene-tetracarboxylic diphenylimide (NTCDI)-derived compounds were already tried in organic devices, including thin and thick film OFETs. The highest mobilities of solution-processed n-type semiconductors were achieved from quaterthiophene ( $0.2 \text{ cm}^2 \text{ V}^{-1} \text{ s}^{-1}$ ) measured in a vacuum and from naphthalene diimide (NTCDI) with a long-chain fluorinated alkyl group ( $0.01 \text{ cm}^2 \text{ V}^{-1} \text{ s}^{-1}$ ) solution-processed in air. The highest n-channel mobilities of these devices, which were based on NTCDI derivatives, were calculated to be about  $1.2 \times 10^{-3} \text{ cm}^2 \text{ V}^{-1} \text{ s}^{-1}$ . A room-temperature electron mobility as high as  $90 \text{ cm}^2 \text{ V}^{-1} \text{ s}^{-1}$  was reported using MLE. Figure 4.10 shows the preliminary results of the characteristics of nano-organic field-effect transistors.

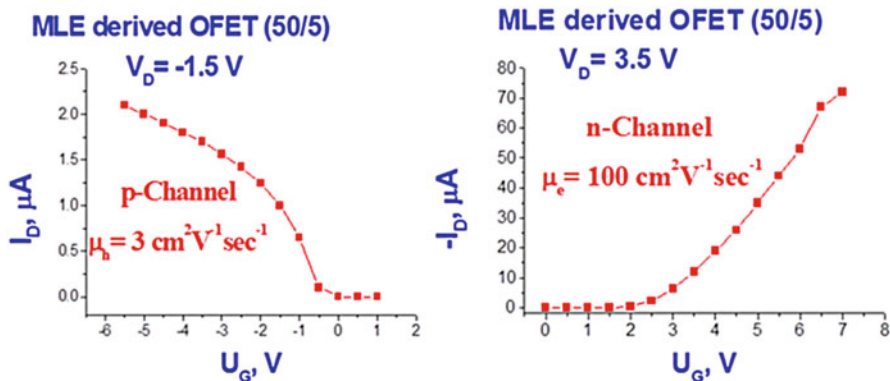


**Fig. 4.10** Mobility charges in bipolar field-effect transistors (nano-OFETs), produced by the MLE technology. The mobility of electrons in the MLE structures reaches 40–200  $\text{cm}^2/\text{Vs}$ , which exceeds the best known values for organic transistors

### 4.3.2 Organic Light-Emitting Diodes produced by MLE technology (MLE-OLEDs)

MLE-derived OLEDs, as small as 4–6 nm thick active layers, were fabricated. Another finite size effect was observed in electroluminescence (EL) of MLE-derived structures. The thickness-dependent EL of  $(\text{NTCDI-DPM})_n$  is depicted in Figure 4.9(b). The EL spectra is shown for an OLED formed by the assembly of 2 and 4 bi-layered NTCDI structures with diphenylmethane (DPM) spacer in a glass/ITO/organic multiply quantum well (OMQW)/Al configuration at a bias of 8 V, where ITO stands for indium tin-oxide electrode. The 480 nm EL maxima for  $(\text{NTCDI-DPM})_n$  was shifted almost 50 nm with doubling of the thickness, and it was clearly observed that two different centers emit under these conditions. The blue EL is attributed to radiative recombination on a single NTCDI molecule and the red EL is assigned to radiative recombination within aggregated NTCDI molecules. The coexistence of two emitting centers within the same layer is an indication that two different excitations exist: (i) intra-molecular excitons and (ii) inter-molecular excitons. The same trend of a new PL peak appearing due to epitaxial ordering (intermolecular excitons) was observed in a single crystal of naphthalene tetracarboxylic di-*n*-hexylimide (NTC-DHI) grown by the Bridgman method. The EL can be shifted to the blue by ramping the applied potential in the same  $(\text{NTCDI-DPM})_n$ , OMQW based devices (Figure 4.9(c)). At low voltage, the red emission of the stacked NTCDI molecules (intermolecular excitons) dominates the EL spectrum, since these centers have a lower energy gap for excitation and charge recombination. Increasing the applied potential leads to charge recombination at the higher energy gap, intramolecular excitons, and to blue-shifted EL. In summary, finite size effects govern blue-shifting of absorption peaks and DC-field EL tunability.



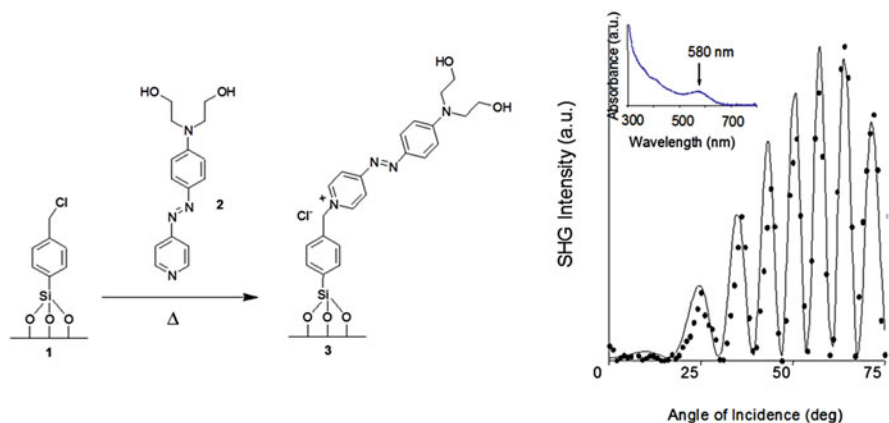


**Fig. 4.11** Example of laser action in MLE structures. Left is a molecular self-assembly in the vapor-gas phase of a precursor (amino-phenyl-azo-pyridinium) on a modified glass substrate. On the right is the generation of the 2nd harmonic upon excitation by light of a wavelength of 1064 nm. The spectrum of the assembled structure is shown on the right side of the inset

### 4.3.3 Laser Media Produced by MLE Method

An example of laser action in MLE structures is shown in Fig. 4.11.

This structure cannot be obtained by liquid-liquid methods due to the insolubility of the precursor (amino-phenyl-azo-pyridinium) and vacuum methodologies that are not capable of creating a chemical bond between the fungicide-bonded silicone substrate and the active molecule. The main characteristic of MLE method is the ability to create stable structures that, from the point of view of their stability, behave in the same way as their inorganic counterparts (e.g., atomic layer epitaxy method).

### 4.3.4 MLE Photovoltaic Cells

The photovoltaic properties of MLE-derived NTCDI structure are exhibited in Fig. 4.12 [28]. The NTCDI structure, which featured in-plane molecular stack system, was assembled on boron-doped silicon wafer. Device configurator is shown at Fig. 4.12a. This measurement enables to evaluate the velocity of redox electron transfer in direction of molecular NTCDI stack (reaction 2 in Fig. 4.11a) and demonstrates the possibility to harvest photo-excited charges at cm-scale distance.

The photovoltage transients consist of voltage rise and decay (Fig. 4.12). The decay is exponential with  $\tau \sim 40 \mu\text{s}$  at the given external load. This component represents the discharge of the cell because of both the backflow and the functional current through the load. The voltage rise originates from accumulation of charges at the anode, and its kinetics depends on the distance between the illuminated spot and silver (Fig. 4.12). To avoid a model bias, we described the kinetics of the voltage rise

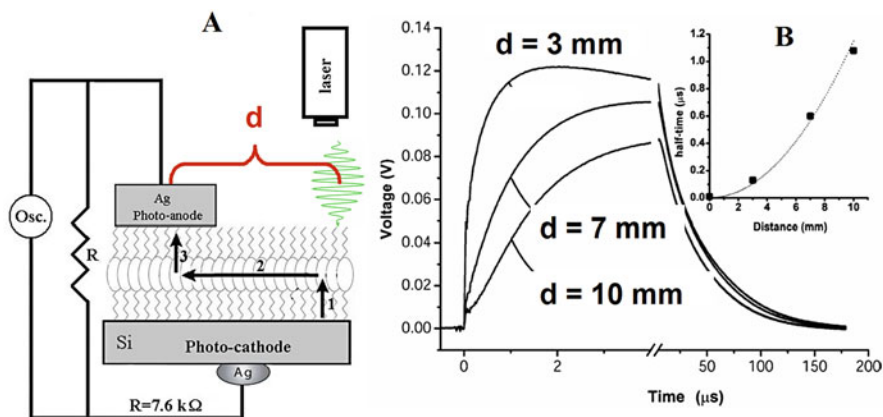


**Fig. 4.12** Scanning time-resolved photovoltage probing. (a) Measurement setup. Distance  $d$  is between illumination point and harvesting upper Ag electrode. The transients were induced by pulses centered at different distances apart from the silver electrode. (b) Kinetic of photoresponse at different  $d$ . The inset shows the dependency of the  $T_{1/2}$  of the voltage rise on the distance between the bright spot and the silver photoanode. The solid line approximates the points by a parabola  $T_{1/2} = l^2/D$  with the parameter  $D \sim 10^6 \text{ cm}^2/\text{s}$

by its halftime  $T_{1/2}$  (Fig. 4.12, inset), which reflects the travel time of the cation radicals. Simple estimate shows that corresponding speed of charge exchange exceeds  $10^4 \text{ m/s}$ . The mutual arrangement of the cell and the incident light; the external quantum efficiency (EQE) of 0.4–0.7 [23], which cannot be accounted for by the absorption efficiency of the film; the dissimilarity of the EQE; and the absorption efficiency of the film and resemblance of EQE to the spectrum of silicon suggest [23] that the light is productively absorbed by the semiconductor (Fig. 4.12). This contrasts with light harvesting in the dye-sensitized photovoltaic cells [29, 30] or the hybrid nanorod-polymer cells [31], which require special junctions with enormous contact areas between the materials to enhance their absorption efficiency. The geometry of the cell also suggests that light harvesting incorporates a longitudinal spatial energy transfer. In contrast to natural photosynthesis [32], the conserved energy does not migrate in the form of excitons. Absorption of light results in elevation of an electron to the conductance band leaving a vacancy in the valence band. This vacancy can be filled either by back recombination of the electron from the conductance band (unproductive decay) or by transfer of an electron from the film into silicon (reaction 1, Fig. 4.12) since the affinity of this vacancy for an electron is apparently high enough to oxidize a molecule of NTCDI. As a result, similarly to the photochemistry of dye-sensitized cells [33, 34], an extra electron remains in the conductance band of silicon, while the oxidized molecules of NTCDI become cation radicals (Fig. 4.12). NTCDA molecules could not be oxidized at normal conditions [35, 36]. It is also known that OFET based on NTCDA molecules shows mobility of  $10^{-4} \text{ cm}^2 \text{ V}^{-1} \text{ s}^{-1}$  [37, 38], while NTCDI-based OFET routinely demonstrates mobilities, which are higher by factor  $10^3$  [39–45].

### 4.3.5 Device Application Scope of MLE Technology

MLE technology was developed in the end of 90th. The initial studies have been concentrated on fabrication of artificial organic superlattices and hybrid heterostructures. The first generation of MLE devices includes MLE-derived organic light-emitting diodes (see Fig. 4.7) and field-effect transistors (see Fig. 4.9). Future development of MLE technology is anticipated along the following directions: artificial photosynthesis (see Fig. 4.12), bi-interfacing, molecular spintronic (see more details on this topic in chapter “Prospects for application of GaAs doped with transition metals as a materials for spintronics” of this book), and nano-lithography technology. Most recent development in MLE devices includes studies toward fabrication of organic NLO devices (see Fig. 4.11), nano-catalytic structures. Figure 4.13 summarizes schematically directions of MLE research development and its device application.

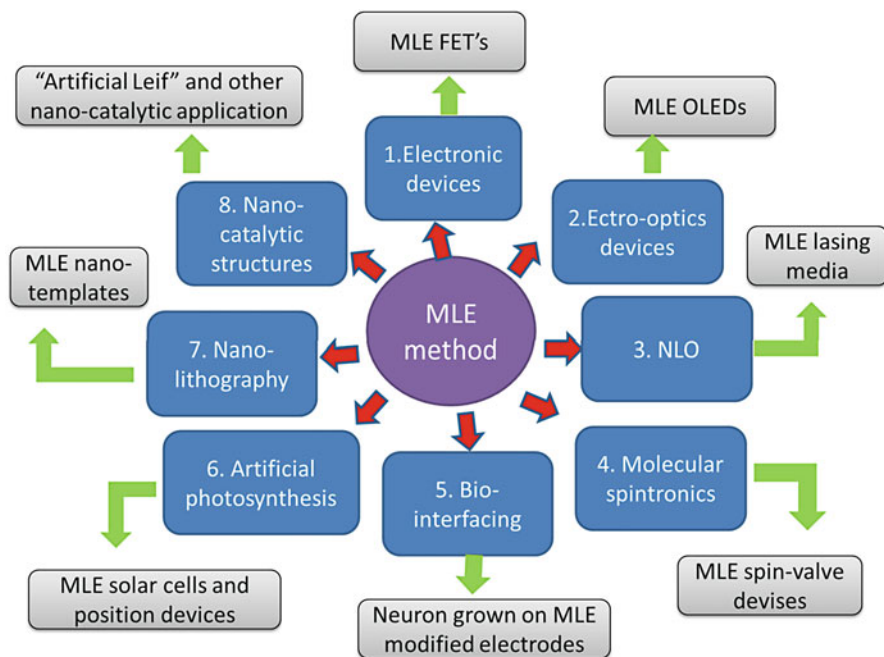


**Fig. 4.13** Application scope of MLE technology. Research directions are shown in blue boxes and device applications are shown in gray boxes

## 4.4 Distinguished Features of MLE Method and Outlook Toward Hybrid Structures

It is instructive to review the characteristic features of MLE technology in respect to other organic thin film technologies to show the potential of the MLE method in molecular nanoelectronics and review its potential directions of development.

### 4.4.1 *Distinguished Features of MLE Method*

We summarize the distinguishing features of MLE method with competing technologies in deposition of organic thin films as follows:

1. MLE is a solvent-free technology. Using of solvents in regular molecular nanoelectronic devices results in decreasing of electronic properties, including charge mobility. This usually is associated with trapping charges on traces of solvent molecules, which remain embedded in matrix of useful electronics material. In addition, any traces of solvents contribute to gradual degradation of useful properties (conductivity, charge mobility, etc.) of molecular electronic device along with degradation of whole device, especially when large operation fields are applied (e.g., due to photooxidation). MLE process is 100% solvent-free technology.
2. MLE enables to employ all kind of precursor materials, regardless of their solubility. All solution-based production methods (solution molecular self-assembly (SAM) films, electrostatic SAM films, LB films, etc.) are limited to molecules, which can be easily dissolved in organic solvents. For example, NTCDA molecule, used in MLE process (see Figs. 4.4 and 4.5), cannot be dissolved in any appreciable amount in solvents for usage in liquid-phase methods.
3. Previous paragraph described MLE to assess new group of organic precursor materials. In addition to this, MLE technology provides a new kind of surface chemistry, which cannot be achieved by liquid- and vapor-phase methods. Indeed, reaction of vapor-phase self-assembly, which is highlighted in Fig. 4.5, is possible only in vapor phase. Even if NTCDA precursor would be soluble in organic solvent, the imidization reaction releases water as a reaction coproduct. The traces of water in liquid phase would react with surface amino groups and prevent growth of organic superlattices (Fig. 4.5). In MLE setup the coproduct is evacuated in vapor phase, which enables the future growth of organic superlattices.
4. MLE method is the only vapor-phase method, which enables self-assembly reactions in vapor phase. Other vapor-phase methods (CVD, UHV, OMBD, etc.) are capable to form only physisorbed films, which are designating sometimes as “pseudo-epitaxy”). These films are characterized by weak intermolecular

bonds, and these films are prone to decompose with time, especially in condition of working devices.

5. While organic superlattices can be achieved by other vapor-phase technologies (e.g., OMBD [18]), the MLE packing of these superlattices is unique as well. Figure 4.4 shows, for example, growth of NTCDI-based superlattices with aliphatic hexa-amine spacers. These superlattices are oriented orthogonally to substrate. OMBD superlattices [41] produced superlattices with NTCDA molecules, which is precursor to NTCDI superlattices in MLE case. There is no example of organic superlattices, which contains lateral  $\pi$ -aggregated moiety produced by solution SAM methods. The capability to create molecular devices with predesigned structures is a distinguished feature of MLE method.

#### ***4.4.2 Outlook for the MLE Method Toward Hybrid Superlattice***

MLE method allows to create materials on the basis of inserted organic-inorganic lattices—structures in which a series of organic layers can be included in a series of inorganic layers. Such structures were never produced and were not investigated. Such hybrid materials can have fundamentally new properties, and the range of their applications is extremely wide: from broadband photodetectors, tandem solar cells, compact energy converters, and hybrid lasers to new classes of solid-state accumulators and nano-generators and to the creation of bio-interfaces. The main characteristic of the 2nd generation of MLE setup is the ability to create stable structures.

#### **Organic-Inorganic Superlattices**

One of the challenging tasks of applied solid-state physics is to develop and study hybrid structures based on organic-inorganic superlattices including AsGa, SiGe, etc., which will be mixed by layers of  $n$ -type organic semiconductors of naphthalene, perylenes, etc. The distinctive feature of these structures will be epitaxial heterostructures, in which organic and inorganic layers will be connected by covalent bonds, which can sustain high temperatures, electrical fields, etc. Mixed heterostructures of this type have enormous potential in electronics and optics as their properties combine features of inorganic semiconductors with organic conducting and semiconducting materials. The possibility to study mixing of molecular properties with the properties of inorganic layers should provide a new level of understanding of solid-state physics. This kind of superlattices and heterostructures can be accomplished only by MLE technology and its derivations. One of the examples of such structure is discussed in the next section.

## Hybrid Perovskite Structures

The hybrid perovskite structures nowadays are considered to be most perspective foundation for new generation of photovoltaic device, which is believed to revolutionize market of solar cells. This development of hybrid solar cell technology can be traced back to experiments with self-assembly of biomolecules on inorganic semiconductors that have been conducted in Berkeley in the 1950s. These studies eventually resulted in appearance of new kind of solar cells, known as dye-sensitizing solar cells or Gratzel cells in 1990, which were based on self-assembly of ruthenium complex on nanoparticles of titanium oxide [31]. These solar cells were the most efficient devices for next 10–15 years, till the hybrid perovskites appeared. Nowadays the hybrid perovskites overwhelm the performance of dye-sensitizing solar cells.

However the nature of electronic processes in hybrid perovskites solar cell device remains unknown, and this impedes the future progress in achieving higher efficiencies. One of the ways to clarify the physics of solar cell device based on hybrid perovskites is to produce and study 2D structures, in which the layer of hybrid perovskites cation (e.g.,  $\text{PbI}_2$ ) can be altered with the hybrid perovskite organic anion (methyl ammonia derivatives). Currently all studies of 2D structures, which contain hybrid perovskites [46], rely on liquid-phase methods. Usage of liquid-phase methods leads in residual of organic solvents along with structural defects (typical for liquid-phase methods) in these 2D hybrid perovskite structures. Application of vapor-phase MLE technology has potential to produce the cleanest and most sophisticated 2D hybrid perovskite structures without molecules of solvents and defects, which are typical for liquid-phase SAM methods. In addition, MLE technology can employ new materials in hybrid perovskite structures, which cannot be used currently due to limited solubility of precursor materials.

## 4.5 Summary

We describe in this chapter a short introduction on new MLE method and summarize the MLE technology in the form of practical tutorial. This tutorial includes demonstration of main principles of MLE technology and few synthetic routes for vapor-phase organic superlattice assembly. Special attention is paid to several fabrication aspects of MLE technology, namely, the combination of *c*-axis bonding and *in-plane* stacking of building motifs, which led to the formation of densely packed and highly regular organic multilayers. The chemical and temporal stability of these organic structures proved to be useful in device operation. Molecular layer epitaxy approaches will be especially applicable in the “heavy duty” fields of molecular electronics, optoelectronics, bioelectronics, as well as fundamental studies.

**Acknowledgments** This research was supported by The Tomsk State University competitiveness improvement program under grant 8.2.20.2018.

## References

1. Reed MA, Zhou C, Muller CJ, Burgin TP, Tour JM (1997) *Science* 278:252
2. Aviram A, Ratner MA (1974) *Molecular Rectifiers*. *Chem Physics* 29:277–283
3. Anelli PL, Spencer N, Stoddart JF (1991) *J Am Chem Soc* 113:5131–5133
4. Petta JR, Slater SK, Ralph DC (2004) *Phys Rev Lett* 93:136601
5. Kelley SO, Barton JK (1999) *Science* 283:375–381
6. Grätzel M (2003) *J Photochem Photobiol C: Photochem Rev* 4:145–153
7. You J, Meng L, Song T-B, Guo T-F, Yang, Y.(M.), Chang W-H, Hong Z, Chen H, Zhou H, Chen Q, Liu Y, De Marco N, Yang Y (2015) *Nat Nanotechnol*:1–9. <https://doi.org/10.1038/nnano.2015.230>
8. Schön JH., [https://en.wikipedia.org/wiki/Schön\\_scandal](https://en.wikipedia.org/wiki/Schön_scandal)
9. Emberly EG, Kirczenow G (2000) *Phys Rev B* 61:5740–5750
10. *Nature Nanotechnology* 8, (2013). <https://doi.org/10.1038/NNANO.2013.91>
11. O'Brien E, Holt ME, Thompson MK, Salay LE, Ehlinger AC, Chazin W, Barton JK (2017) *Science* 355:1789
12. <https://www.theverge.com/2016/8/1/12340454/gsk-google-bioelectronic-medicine-company>
13. <https://www.wsj.com/articles/elon-musk-launches-neuralink-to-connect-brains-with-computers-1490642652>
14. Kopylova TN, Nikonov SU, Telminov EN, Gadirov RM, Degtyarenko KM, Burtman V (2016) chapter 1. In: Jensen K (ed) *Heterogeneous catalysts*. Nova publishers, New York, pp 1–21
15. Zhang Y, Xu L, Walker WR, Tittle CM, Backhouse CJ, Pope MA (2017) *J Mater Chem C* 43:13
16. Ulman A (1991) *An introduction to ultrathin organic films*. Boston, Academic Press
17. Yao Q, Luo Z, Yuan X, Yu Y, Zhang C, Xie J, Lee JY (2014) *Sci Rep* 4:3848
18. Zimmerman JD, Lassiter BE, Xiao X, Sun K, Dolocan A, Gearba R, Vanden-Bout DA, Stevenson KJ, Wickramasinghe P, Thompson ME, Forrest SR (2013) *ACS Nano* 7:9268
19. Kiy M, Suhner U, Gamboni I, Gunter P, Biaggio I (2000) *Synth Met* 111:307–310
20. Tubino R, Borghesi A, Dalla BL, Destrid S, Porziod W, Sassella A (1998) *Opt Mater* 9:437–444
21. Puurunen RL (2014) A short history of atomic layer deposition: Tuomo Suntola's atomic layer epitaxy (essay). *Chem Vap Depos* 20:332–334
22. Burtman V, Zelichenok A, Yitzchaik S (1999) *Angew Chem Int Eng Ed* 38:2041
23. Whitesides GM, Laibinis PE (1990) *Langmuir* 6:87
24. Burtman V, Ofir Y, Yitzchaik S (2001) *Langmuir* 17:2137
25. Burtman V, Vardeny ZV (2008) *Jpn J Appl Phys* 47:1165–1172
26. Yitzchaik S, Marks TJ (1996) *Acc Chem Res* 29:197–202
27. Burtman V (2012) In: Antsyforov GI, Ivanski AF (eds) *Naphthalene: structure, properties and applications*, chapter 1. Nova Publishers, New York, pp 1–58
28. Zaslavsky D, Pakoulev AV, Burtman V (2004) *J Phys Chem B* 108:15815
29. Sze S (1985) *Semiconductor devices physics and technology*. Wiley, New York
30. Hagfeldt A, Gratzel M (2000) *Acc Chem Res* 33:269
31. Grätzel M (2001) *Nature* 414:338
32. Huynh WU, Dittmer JJ, Alivisatos AP (2002) *Science* 295:2425
33. Glazer AN (1983) *Annu Rev Biochem* 52:125
34. Di Bilio AJ, Crane BR, Wehbi WA, Kiser CN, Abu-Omar MM, Carlos RM, Richards JH, Winkler JR, Gray HB (2001) *J Am Chem Soc* 123:3181
35. Burtman V, Zelichonok A, Pakoulev AV (2011) *Int J Mol Sci* 12:173–225
36. Coropceanu V, Cornil J, da Silva-Filho DA, Olivier Y, Silbey R, Bredas J-L (2007) *Chem Rev* 107:926
37. Laquindanum JG, Katz HE, Dodabalapur A, Lovinger AJ (1996) *J Am Chem Soc* 118:11331
38. Tanida S, Noda K, Kawabata H, Matsushige K (2009) *Thin Solid Films* 518:571
39. Facchetti A (2007) *Mater Today* 10:28
40. Katz HE, Johnson J, Lovinger AJ, Li W (2000) *J Am Chem Soc* 122:7787

41. Singh TB, Erten S, Günes S, Zafer C, Turkmen G, Kuhan B, Teoman Y, Sariciftci NS, Icli S (2006) *Org Electron* 7:480
42. Kao CC, Lin P, Lee CC, Wang YK, Ho JC, Shen YY (2007) *Appl Phys Lett* 90:212101
43. Letizia JA, Facchetti A, Stern CL, Ratner MA, Marks TJ (2005) *J Am Chem Soc* 127:13476
44. Lee Y-L, Hsu H-L, Chen S-Y, Yew T-R (1694) *J Phys Chem C* 112:2008
45. Janssen D (2006) Long-term performance versus structure of polymer materials. Ph.D. thesis, Katholieke University of Leuven, Belgium
46. Du K-z, Tu Q, Zhang X, Han Q, Liu J, Zauscher S, Mitzi DB (2017) *Inorg Chem* 56:9291–9302